

Multi-Modal Image Fusion via Integrated Anisotropic Diffusion in Stationary Wavelet Domain

¹Bhawna Goyal, ²Ayush Dogra, ³Rahul Khoond , ⁴Kanav Sharma
^{1,3,4}ECE, Chandigarh University, Gharuan Mohali
²UIET, Panjab University, Chandigarh

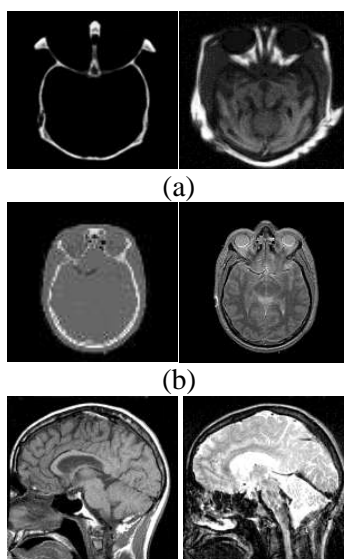
Abstract

CT and MR scans are used in medical imaging to capture the information of targeted organs. For better diagnosis these two models have to be combined into a single frame. Image fusion is a technique of generating proficient or interesting information from a set of source images. Fusion method is used to obtain the maximum information with least information loss in a single image. A new fusion method is proposed for medical imaging where anisotropic diffusion is used to exclude source image into approximation and detail layer. Guided filter is used to preprocess the excluded source images beside with the help of stationary wavelet transform and weighted linear superposition final fused image is obtained. Petrovic metrics are applied to assess the execution of the proposed method. The obtained results show that the proposed method outperforms the other state of art method.

Keywords- Image Fusion, Wavelet, Anisotropic diffusion, Guided Filter

INTRODUCTION

In the field of medical science, images are taken for CT and MRI used for getting corresponding data. Hard tissue data like bone structure is provided by CT image (left side) whereas soft data like flesh is provided by MRI image (right side) which is shown in Figure 1. But for the better treatment of the patients, doctor needs single image information of CT and MRI. As we know that single sensor image is not able to capture or provide complete data of a particular scene by cause of sensor system disadvantage. To overcome this problem, different types of images are bundled together to form a single image for providing useful information of an image. Image fusion is a technique which is used to merge important information from many taken images of a particular scene into a single image which provides more information of a scene. Thus, the needed information from various sensing devices is combining into a particular image. Over the last years many researchers are attracted toward image fusion [1] because of its many applications. These are some application areas of image fusion such as remote sensing [2], weapon detection [3], digital photography [4], helicopter navigation [5], medical imaging, navigation and military [6], [7], [8], [9], [10]. With the help of image fusion it is easy to get a single image with useful information that is needed or required. It makes the human work easy [11].



(c)
FIGURE 1: (a) Data 1, (b) Data 2 and (c) Data 3 – CT and MRI Images

RELATED WORK

There are usually three processing levels for image fusion and they are based on signal, feature and decision levels. The other name for signal level image fusion is pixel level image fusion and it is related to each unique pixel from various number of images into a fused image. Signal level image fusion is much border area of multisensory and multifocus fusion, besides many researcher has attracted toward it [12-15]. Feature level image fusion is the other name of object level image fusion and it deals fusion of features along with object labels and property figures which have been extracted from source images [16]. Decision or symbol based fusion deals fusion of probabilistic information which has obtained from data with the help of object level processing [17].

Multifocus and multispectral image fusion has been carried out by many researchers which is based on intensity has saturation method as discussed in [18] and Laplacian pyramid based on [19, 20]. Further fusion method based on wavelet transform proposed by [21-25, 26]. In [25], medical image fusion is discussed based on wavelet transform, lifting based wavelet as proposed in [26] to reduce the complexity and memory requirement. Introduction of complex wavelet for image fusion have upgraded the fusion performance [27]. Satellite image fusion using multi-scale wavelet is proposed in [24] and fusion methods discussed in literature are differentiated with [29]. Image fusion relying upon sequence support value along with low frequency images has been discussed in [30]. And, signal level multifocus image fusion is built on image blocks and artificial neural network [31]. Also pixel level fusion introduce decomposition of source image using wavelet, wavelet packet [42] and contoured transform [18, 32]. DCT based image fusion has been discussed in [33]. The bilateral filter (BF) proposed by [34] has application in image denoising [35, 36, 37], hash photography [38, 39], image/videos fusion [40, 41] etc.

METHODOLOGY

Image fusion algorithm separates the source image (CT and MRI) into its detail layer and base layer using anisotropic diffusion technique.

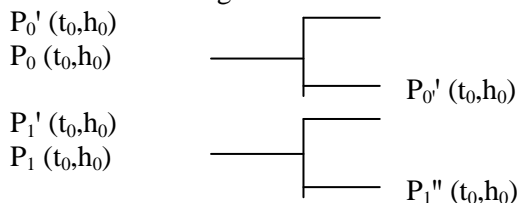
$P_n(t_0, h_0)$; $n \geq 0, 1$, $P_n(t_0, h_0)$ is a source image.

Whereas

$P_0(t_0, h_0)$ is CT image &

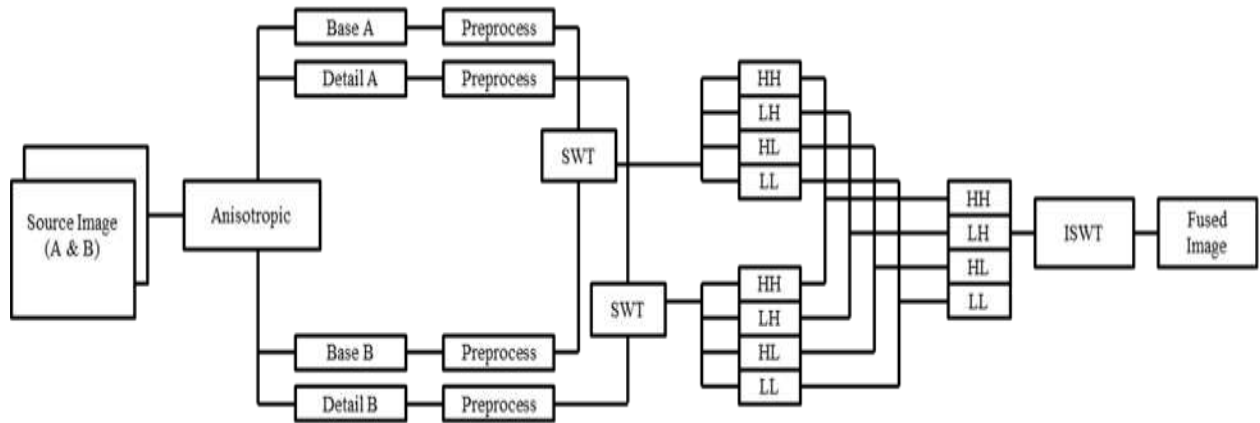
$P_1(t_0, h_0)$ is MRI image

The excluded base and detail layer of each (CT & MRI) is preprocessed using guided filter which evaluated the images and remove the artifacts presents.



Where $P_0'(t_0, h_0)$ and $P_0''(t_0, h_0)$ excluded base and detail layer of CT image. Similarly $P_1'(t_0, h_0)$ and $P_1''(t_0, h_0)$ excluded base and detail layer of MRI image. The stationary wavelet transform which is used for generating the fused image into a single image. The whole methodology is designed in figure 2. Each step of the method is elaborated in detail in the following sub categories.

- A. Anisotropic diffusion
- B. Preprocessing using guided filter
- C. Fusion using stationary wavelet transform



(A) Anisotropic diffusion

The process of anisotropic diffusion uses partial differentiation equation (PDE) to smooth the homogeneous region of an image while protecting the non homogeneous region (edges) besides it represses the deficiency of isotropic diffusion which uses inter-region refinement due to which edge information is irretrievable. To overcome the loss anisotropic diffusion is introduced which use intra-region smoothing to enhance the resolution of an image while processing the edges. The anisotropic diffusion we flex function to curb the diffusion as

$$Pt = D(t, h, t) \Delta P + \nabla D \cdot \nabla P \text{---- (1)}$$

Where, Pt = source image, $D(t, , t)$ = flex function or diffusion rate, Δ = Laplacian operator, ∇ = Gradient operator, t = number of iteration.

In another way forward-time-central-space (FTCS) scheme is applied to evaluate the equation 1. Hence PDE becomes

$$Pi, j^{t+1} = Pi, j^t + \lambda [Dn. \delta n Pi^t, j + Ds. \delta s Pi^t, j + De. \delta e Pi^t, j + Dw. \delta w Pi^t, j] \text{---- (2)}$$

Pi, j^{t+1} = resolution of an image at $t+1$ iteration, λ is a stability constant lies between 0, 1/4. $\delta n, \delta s, \delta e$ and δw are the nearest neighbor in all direction and they are defined as

$$\delta n Pi, j = Pi - 1, j - Pi, j ,$$

$$\delta s Pi, j = Pi + 1, j - Pi, j ,$$

$$\delta e Pi, j = Pi, j + 1 - Pi, j ,$$

$$\delta w Pi, j = Pi, j - 1 - Pi, j \text{---- (3)}$$

Similarly, Dn, Ds, De and Dw are flux function in all directions.

$$D_{Ni, j}^t = H(\|(\delta P)_{i+1/2, j}^t\|) = H(|\delta n P_{i, j}^t|),$$

$$D_{Si, j}^t = H(\|(\delta P)_{i-1/2, j}^t\|) = H(|\delta s P_{i, j}^t|),$$

$$D_{Ei, j}^t = H(\|(\delta P)_{i, j+1/2}^t\|) = H(|\delta e P_{i, j}^t|),$$


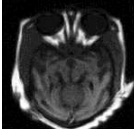
$$D_{Wi, j}^t = H(\|(\delta P)_{i, j-1/2}^t\|) = H(|\delta w P_{i, j}^t|) \text{---- (4)}$$

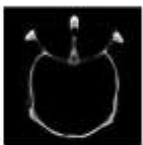
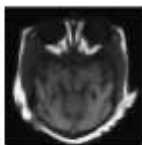


In (4), $H(|\delta w P_{i, j}^t|)$ is a descending function with $H(0) = 1$. To exclude the base layer and detail layer, let source images $[Pn(t, h)]_{n=1}^N$ are of size $m \times n$. Using anisotropic diffusion process on these images base layer is obtain as

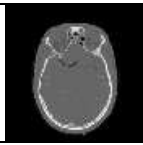
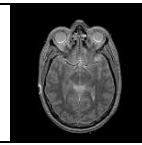
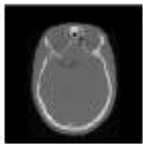
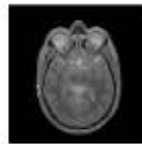


$$Bn(t, h) = \text{anist}(Pn(t, h)),$$

Where $Bn(t, h)$ is n th base layer and $\text{anist}(Pn(t, h))$ is n th process anisotropic diffusion. Detail layer are possessed by subtracting base layer from the source images.

$$Dn(t, h) = Pn(t, h) - Bn(t, h).$$

Dataset a	CT	MRI
Images		

Base Layer		
Detail Layer		

Dataset b	CT	MRI
Images		
Base Layer		
Detail Layer		

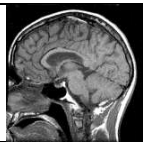
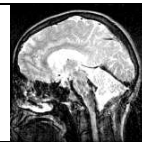




Dataset c	CT	MRI
Images		
Base Layer		
Detail Layer		

FIGURE 3:representing the obtained base and detail layer.

(B) Preprocessing using guided filter

Guidedfilter (GF) is an obvious image filter. Here the statistics of the neighboring pixels are taken for counting the pixels of an image. It enumerates output similar to any other linear time invariant (LTI) filter but it use secondary image to filter the primary image or input image. Secondary image could be same as that of the input image or it can be a translated version of the input image. Guided filter is edge preserving filter beside it doesn't only prevent the edges rather it smooth the image as shown mathematically => the filter output F_p is given by

$$F_p = M_i H_j + n_i, \forall_j \in w_i, \text{--- (1)}$$

Where, H_j guided image at pixel in a square of window w_l , m_l and n_l are linear coefficients of window m_l and n_l . In order to get the noise free image. Noise image is subtracted from input image. Therefore,

$$F_p = P_j - D_j \text{--- (2)}$$

By taking the minimum value of P and D . The minimum function of $F(m_l, n_l)$ can be written as

$$F(m_l, n_l) = \sum (m_l H_j + n_l - I_j)^2 + \epsilon M L^2 \text{--- (3)}$$

Where ϵ is the regularization parameter. Equation can be written as

$$M_l = \frac{\frac{1}{|w_l|} \sum H_i I_j - \mu_i T_l}{\sigma_l^2 + \epsilon} \text{--- (4)}$$

$$\eta_l = T_l - M_l H_l$$

W = number of pixel in window,

U_l = means, σ_l^2 = variance of window W_l .

T_l = mean of input.

By solving the equation 2, 3, 4 the filtering output can be written as

$$F_p \xrightarrow{M_i} G_i \xrightarrow{\eta_i}$$

If the variance of the guidance image is higher than its threshold, $\epsilon(\sigma_l^2) \geq \epsilon$ then the central pixel remains unchanged whereas if the variance is low pixel value is replaced by the average of neighboring pixel.

(C) Fusion using stationary wavelet transforms

Stationary wavelet transform doesn't involve decimation. Therefore number of samples for input signal is half that of its coefficient. From figure it is clear that it excludes an image pixel into different sub-bands i.e. LL, LH, HL and HH depicting low resolution approximation, horizontal, vertical and diagonal detail.

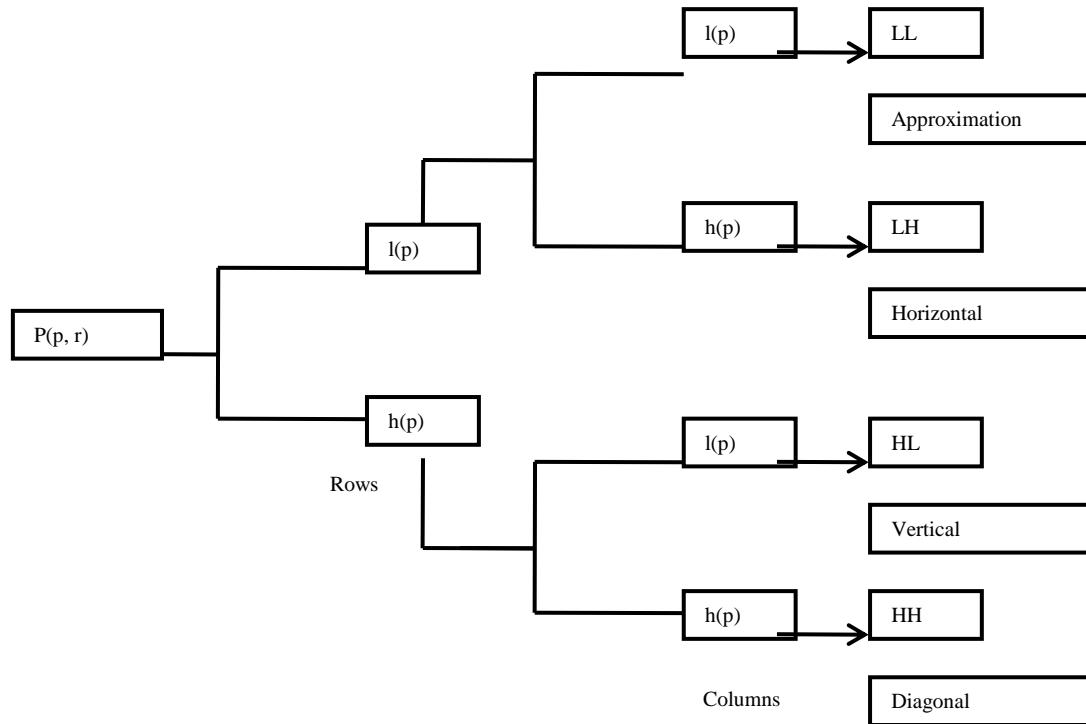


FIGURE 4:Fusion using stationary wavelet transforms

Once the source image is dissolved into its sub image bands the mean approximate part of an image is taken and horizontal detail layer of second part is subtracted from first part. This can be seen as

$$D = (\text{abs}(H1L1) - \text{abs}(H2L2)) \geq 0$$

Similarly, the calculation for approximate vertical detail layer is obtained and it is written as

$$D = (\text{abs}(V1L1) - \text{abs}(V2L2)) \geq 0$$

Fusion of horizontal part is multiplication of horizontal detail of first image subtracted from multiplication of detail of second image and inverse stationary wavelet transform (ISWT) will be used for calculating the approximate fused image.

RESULT AND DISCUSSION:

Experimental result is obtained by medical images (CT and MRI) which are taken from [39]. The trails are implemented on Intel i5 core CPU-2.50GHz processor with 4Gb RAM where the image resolution is 256x256. The parameter used for proposed method are $r=25$ and $w=5$. The output of proposed method is fusion result of LL, HL, LH, HH layer of both base layer and detail layer. Fusion is done using SWT besides ISWT provides the final output image. Anisotropic diffusion excludes the image into its base layer and detail layer. Once the layer are excluded guided filter preprocess these layer feed the result into SWT.

To differentiate the performance visually, the integrated MRI and CT images are shown in figure 5. As shown in the figures A, B source images and proposed method in (C). Anisotropic diffusion techniques are compared to proposed natural and qualitative, quantitative performance is shown in fig1, fig 2, fig 3, table 1 respectively. Quantitative performance consists of Qab/f , Lab/f , Nab/f . Where Qab/f , is total information transformed from source image to final image and it is given as Qab/f , is fusion gain and Lab/f is total information loss and Nab/f is noise and artifacts added in fused image. Nab/f is given as

$$Nab/f = \frac{\sum_u \sum_v \sum_u A M u v [(1 - Q_{u,v}^{AF}) W_{u,v}^A + (1 - Q_{u,v}^{BF}) W_{u,v}^B]}{\sum_u \sum_v \sum_u (W_{u,v}^A + W_{u,v}^B)}$$

Where,

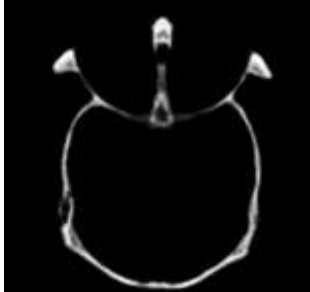

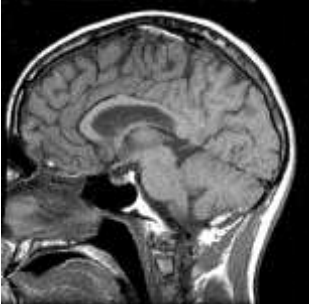
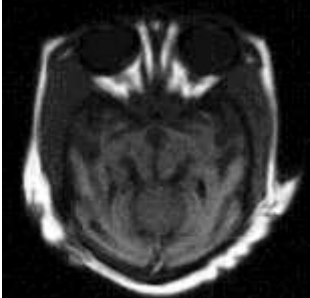

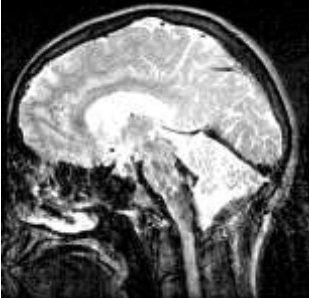
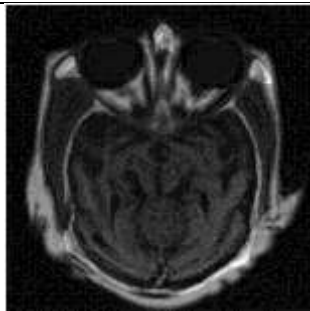


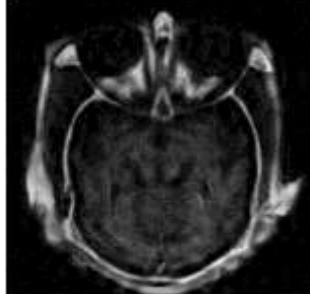

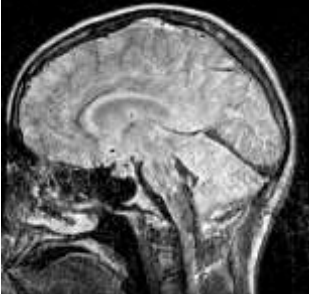
$AMij = \{1, g_{u,v}^F > g_{u,v}^A \text{ and } g_{u,v}^F > g_{u,v}^B, \text{ represent location of artifacts}\}$
 $\infty, \text{ otherwise}$

It is noted that, sum of $Qab/f, Lab/f, Nab/f$ is equal to 1.

Therefore,

$$Qab/f + Lab/f + Nab/f = 1$$

It is observed from figure 5 that the property of integrated image is better than the other method. Considered and has all detail from source image with high fusion rate and information loss.

Dataset	A	B	C
CT Images			
MRI Images			
ADF			
DCHWT Image Fusion Codes			

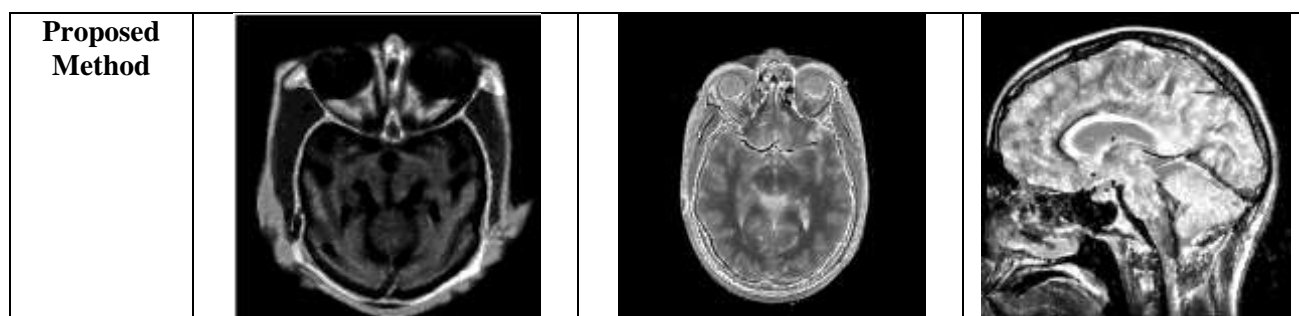


Figure 5

PETROVIC METRICS	FUSION SCORE (QABF)	FUSION LOSS (LABF)	FUSION ARTIFACTS (NABF)
ADF	0.5344	0.4497	0.0908
DCHWT Image Fusion Codes	0.5901	0.3773	0.1250
Ours	0.5922	0.3461	0.2835

Petrovic metrics for Dataset (a) from figure 5

PETROVIC METRICS	FUSION SCORE (QABF)	FUSION LOSS (LABF)	FUSION ARTIFACTS (NABF)
ADF	0.5177	0.4287	0.1832
DCHWT Image Fusion Codes	0.5194	0.4512	0.1056
Ours	0.6047	0.3070	0.3077

Petrovic metrics for Dataset (b) from figure 5

PETROVIC METRICS	FUSION SCORE (QABF)	FUSION LOSS (LABF)	FUSION ARTIFACTS (NABF)
ADF	0.4417	0.5267	0.0858
DCHWT Image Fusion Codes	0.7129	0.2693	0.0614
Ours	0.5004	0.4041	0.2672

Petrovic metrics for Dataset (c) from figure 5

CONCLUSION

We have proposed fusion method for medical images (CT and MRI). First, source images are diffused into base layer and detail layer using anisotropic diffusion techniques these excluded layers and preprocessed using guided filter and fused using stationary wavelet transform. Evolution metrics performance results shows that proposed method is well compatible for medical image fusion beside it shows promising results compared to traditional and recent fusion technique. The performance of proposed method can be enhanced by exploring the other methods and further it can be modified to fuse multiple source images.

Acknowledgement: This experimental work has been jointly carried out by Chandigarh University and UIET, ECE, Panjab University during the year 2018-19.

REFERENCE:

1. Bavirisetti, D.P. and Dhuli, R., 2015. Fusion of infrared and visible sensor images based on anisotropic diffusion and Karhunen-Loeve transform. *IEEE Sensors Journal*, 16(1), pp.203-209.
2. Chen, S., Zhang, R., Su, H., Tian, J. and Xia, J., 2010. SAR and multispectral image fusion using generalized IHS transform based on à trous wavelet and EMD decompositions. *IEEE Sensors Journal*, 10(3), pp.737-745.
3. Jameel, A., Ghafoor, A. and Riaz, M.M., 2014. Adaptive compressive fusion for visible/IR sensors. *IEEE Sensors Journal*, 14(7), pp.2230-2231.
4. Shen, R., Cheng, I., Shi, J. and Basu, A., 2011. Generalized random walks for fusion of multi-exposure images. *IEEE Transactions on Image Processing*, 20(12), pp.3634-3646.
5. Rockinger, O., 1999. Multiresolution-Verfahren zur fusion dynamischer bildfolgen. dissertation. de.
6. Kumar, B.S., 2015. Image fusion based on pixel significance using cross bilateral filter. *Signal, image and video processing*, 9(5), pp.1193-1204.
7. Kumar, B.S., 2013. Multifocus and multispectral image fusion based on pixel significance using discrete cosine harmonic wavelet transform. *Signal, Image and Video Processing*, 7(6), pp.1125-1143.
8. Li, S. and Yang, B., 2010. Hybrid multiresolution method for multisensor multimodal image fusion. *IEEE Sensors Journal*, 10(9), pp.1519-1526.
9. Mitianoudis, N. and Stathaki, T., 2008. Optimal contrast correction for ICA-based fusion of multimodal images. *IEEE sensors journal*, 8(12), pp.2016-2026.
10. Naidu, V.P.S., 2011. Image fusion technique using multi-resolution singular value decomposition. *Defence Science Journal*, 61(5), pp.479-484..
11. Blum, R.S. and Liu, Z. eds., 2005. Multi-sensor image fusion and its applications. CRC press.
12. Li, H., Manjunath, B.S. and Mitra, S.K., 1995. Multisensor image fusion using the wavelet transform. *Graphical models and image processing*, 57(3), pp.235-245.
13. Ben Hamza, A., He, Y., Krim, H. and Willsky, A., 2005. A multiscale approach to pixel-level image fusion. *Integrated Computer-Aided Engineering*, 12(2), pp.135-146.
14. Shah, P., Merchant, S.N. and Desai, U.B., 2013. Multifocus and multispectral image fusion based on pixel significance using multiresolution decomposition. *Signal, Image and Video Processing*, 7(1), pp.95-109.
15. Shah, P., Merchant, S.N. and Desai, U.B., 2013. Multifocus and multispectral image fusion based on pixel significance using multiresolution decomposition. *Signal, Image and Video Processing*, 7(1), pp.95-109.
16. Sasikala, M. and Kumaravel, N., 2007. A comparative analysis of feature based image fusion methods. *Information Technology Journal*, 6(8), pp.1224-1230.
17. Tao, Q. and Veldhuis, R., 2009. Threshold-optimized decision-level fusion and its application to biometrics. *Pattern Recognition*, 42(5), pp.823-836.
18. CARPER, W., LILLESAND, T. and KIEFER, R., 1990. The use of intensity-hue-saturation transformations for merging SPOT panchromatic and multispectral image data. *Photogrammetric Engineering and remote sensing*, 56(4), pp.459-467.
19. Toet, A., 1990. Hierarchical image fusion. *Machine Vision and Applications*, 3(1), pp.1-11.
20. Qu, G., Zhang, D. and Yan, P., 2001. Medical image fusion by wavelet transform modulus maxima. *Optics Express*, 9(4), pp.184-190.
21. S. Singh, N. Mittal, and H. Singh, "Multifocus Image Fusion Based on Multiresolution Pyramid and Bilateral Filter," *IETE J. Res.*, 2020.
22. H. Kaur, K. Kaur, and N. Taneja, "Pixel Level Image Fusion Using Different Wavelet Transforms on Multisensor&Multifocus Images," *Lect. Notes Networks Syst.*, vol. 46, pp.

- 479–488, 2019.
23. U. Shafi and S. Sharma, "Ovarian Cancer Detection in MRI Images using Feature Space and Classification Method (ABC-CNN)," *Int. J. Recent Technol. Eng.*, vol. 8, no. 2 Special Issue 6, pp. 545–551, 2019.
24. D. Kaur and S. Singh, "Detection of brain tumor using image processing techniques," *Int. J. Eng. Adv. Technol.*, vol. 8, no. 5 Special Issue 3, pp. 501–504, 2019.
25. Zhi-guo, J., Dong-bing, H., Jin, C. and Xiao-kuan, Z., 2004, December. A wavelet based algorithm for multi-focus micro-image fusion. In *Third International Conference on Image and Graphics (ICIG'04)* (pp. 176-179). IEEE.
26. Ranjith, T. and Ramesh, C., 2001. A lifting wavelet transform based algorithm for multi-sensor image fusion. *CRL Tech. J.*, 3(3), pp.19-22.
27. Hill, P.R., Canagarajah, C.N. and Bull, D.R., 2002, September. Image Fusion Using Complex Wavelets. In *BMVC* (pp. 1-10).
28. Du, Y., Vachon, P.W. and Van der Sanden, J.J., 2003. Satellite image fusion with multiscale wavelet analysis for marine applications: preserving spatial information and minimizing artifacts (PSIMA). *Canadian Journal of Remote Sensing*, 29(1), pp.14-23.
29. Wang, Z., Ziou, D., Armenakis, C., Li, D. and Li, Q., 2005. A comparative analysis of image fusion methods. *IEEE transactions on geoscience and remote sensing*, 43(6), pp.1391-1402.
30. Zheng, S., Shi, W.Z., Liu, J., Zhu, G.X. and Tian, J.W., 2007. Multisource image fusion method using support value transform. *IEEE Transactions on Image Processing*, 16(7), pp.1831-1839.
31. Li, S., Kwok, J.T. and Wang, Y., 2002. Multifocus image fusion using artificial neural networks. *Pattern Recognition Letters*, 23(8), pp.985-997.
32. Shah, P., Srikanth, T.V., Merchant, S.N. and Desai, U.B., 2011, June. A novel multifocus image fusion scheme based on pixel significance using wavelet transform. In *2011 IEEE 10th IVMSWP Workshop: Perception and Visual Signal Analysis* (pp. 54-59). IEEE.
33. Naidu, V.P.S., 2010. Discrete cosine transform-based image fusion. *Defence Science Journal*, 60(1), pp.48-54.
34. Tomasi, C. and Manduchi, R., 1998, January. Bilateral filtering for gray and color images. In *Sixth international conference on computer vision (IEEE Cat. No. 98CH36271)* (pp. 839-846). IEEE.
35. Zhang, M. and Gunturk, B.K., 2008. Multiresolution bilateral filtering for image denoising. *IEEE Transactions on image processing*, 17(12), pp.2324-2333.
36. Mustafa, Z.A. and Kadah, Y.M., 2011, February. Multi resolution bilateral filter for MR image denoising. In *2011 1st Middle East Conference on Biomedical Engineering* (pp. 180-184). IEEE.
37. Kumar, B.S., 2013. Image denoising based on non-local means filter and its method noise thresholding. *Signal, image and video processing*, 7(6), pp.1211-1227.
38. Petschnigg, G., Szeliski, R., Agrawala, M., Cohen, M., Hoppe, H. and Toyama, K., 2004. Digital photography with flash and no-flash image pairs. *ACM transactions on graphics (TOG)*, 23(3), pp.664-672.
39. Eisemann, E. and Durand, F., 2004. Flash photography enhancement via intrinsic relighting. *ACM transactions on graphics (TOG)*, 23(3), pp.673-678.
40. HU JW, L.I.S.T., 2012. The multiscale directional bilateral filter and its application to multisensor image fusion. *Inform Fu-sion*, 13(3), pp.196-206.
41. Bennett, E.P., Mason, J.L. and McMillan, L., 2007. Multispectral bilateral video fusion. *IEEE Transactions on Image Processing*, 16(5), pp.1185-1194.
42. Shah, P., Merchant, S.N. and Desai, U.B., 2010. Fusion of surveillance images in infrared and visible band using curvelet, wavelet and wavelet packet transform. *International Journal of Wavelets, Multiresolution and Information Processing*, 8(02), pp.271-292.
43. <https://drive.google.com/drive/folders/OBzXT0LnoyRqleHhrdZE3UUVzdVE> (Accessed on 15.10.2018)